Clim. Past Discuss., 11, 63–93, 2015
www.clim-past-discuss.net/11/63/2015/
doi:10.5194/cpd-11-63-2015

Climate of the Past Discussions
Open Access

Strong winter monsoon wind causes surface cooling over India and China in the Late Miocene

H. Tang[1], J. T. Eronen[1,2], A. Kaakinen[1], T. Utescher[3], B. Ahrens[4], and M. Fortelius[1]

[1]Department of Geosciences and Geography, University of Helsinki, P.O. Box 64, 00014, Helsinki, Finland
[2]Biodiversity and Climate Research Centre (BiK-F), Senckenberganlage 25, 60325 Frankfurt am Main, Germany
[3]Senckenberg Research Institute, Frankfurt Main; Steinmann Institute, University of Bonn, Nussallee 8, 53115 Bonn, Germany
[4]Institute for Atmospheric and Environmental Sciences, Goethe University, Altenhoeferallee 1, 60438, Frankfurt am Main, Germany

Received: 26 November 2014 – Accepted: 29 December 2014 – Published: 23 January 2015

Correspondence to: H. Tang (hui.tang@helsinki.fi)

Published by Copernicus Publications on behalf of the European Geosciences Union.

Abstract

Modern Asian winter monsoon characterised by the strong northwesterly wind in East Asia and northeasterly wind in South Asia, has a great impact on the surface temperature of the Asian continent. Its outbreak can result in significant cooling of the monsoon region. However, it is still unclear whether such an impact existed and is detectable in the deep past. In this study, we use temperature reconstructions from plant and mammal fossil data together with climate model results to examine the co-evolution of surface temperature and winter monsoon in the Late Miocene (11–5 Ma), when a significant change of the Asian monsoon system occurred. We find that a stronger-than-present winter monsoon wind might have existed in the Late Miocene due to the lower Asian orography, particularly the northern Tibetan Plateau and the mountains north of it. This can lead to a pronounced cooling in southern China and northern India, which counteracts the generally warmer conditions in the Late Miocene compared to present. The Late Miocene strong winter monsoon was characterised by a marked westerly component and primarily caused by a pressure anomaly between the Tibetan Plateau and Northern Eurasia, rather than by the gradient between the Siberian High and the Aleutian Low. As a result, the close association of surface temperature with winter monsoon strength on inter-annual scale as observed at present may not have established in the Late Miocene.

1 Introduction

Modern surface temperature in Asia is strongly modulated by the strength of winter monsoon, i.e., northwesterly (northeasterly) wind over East Asia (India). As shown in Fig. 1a, strong winter monsoon years as depicted by enhanced low-level northerly wind in East Asia, are associated with an extensive decline of winter temperature in East Asia and India due to cold air mass advection brought by the winter monsoon wind. Also accompanying the strong winter monsoon wind is a strengthened Siberian

High and Aleutian Low (Fig. 1a) and a dipole change of the zonal wind in the upper troposphere (Fig. 1b) indicating an enhanced westerly jet stream and monsoon trough over East Asia. How the surface temperature in Asia had been influenced by the winter monsoon strength in deep geological times, however, is largely unknown.

While the existence of the Asian winter monsoon can be traced back to the Eocene (Licht et al., 2014), the Late Miocene (11–5 Ma) is still an important period with significant changes of the Asian monsoon system documented by various geological records (An et al., 2001; Fortelius et al., 2002; Wang et al., 2005; Molnar et al., 2010). Large uncertainties still remain regarding the relative strength of winter monsoon in this period (Tang et al., 2011). Most studies have suggested a weak winter monsoon in the Late Miocene (Guo et al., 2002; Jia et al., 2003; Wan et al., 2007; Jiang and Ding, 2010; Jacques et al., 2013; Lu and Guo, 2014). They attributed this to the lower elevation of the Tibetan Plateau (TP) and the absence of the northern hemispheric ice sheet in the Late Miocene, both of which has been shown by climate models to favour a weaker Siberian High and a dampened winter monsoon wind (Kutzbach et al., 1993; An et al., 2001; Liu and Yin, 2002; Zhang et al., 2014). Conversely, there are some studies indicating a strong winter monsoon (or winter monsoon dominated climate) in the Late Miocene or even earlier periods (Vandenberghe et al., 2004; Li et al., 2008, 2014; Quan et al., 2012; Zhang et al., 2012), requiring different mechanisms to explain these changes. Better knowledge on temperature changes over the Asian monsoon region and its association with the winter monsoon strength in the Late Miocene would provide useful insights into the evolution of the winter monsoon system and its driving mechanisms at this period.

In this study, we synthesize quantitative reconstructions of the Late Miocene temperature over the Asian monsoon region from two independent proxies, and compare them with climate model simulations of the Late Miocene. We show that the winter temperature in southern China and northern India might have been lower-than-present in the Late Miocene, owing to a strong winter monsoon wind caused by the lower elevation of the northern TP and the mountains north of it. The strong winter monsoon was characterised by a marked westerly component caused by a pressure anomaly between the TP and Northern Eurasia, while the modern-like Siberian High driven winter monsoon system may not have been fully established in this period.

2 Materials and methods

2.1 Temperature reconstruction from proxy records

In this study, we use temperature reconstructions based on plant and mammal fossil records from the Late Miocene localities in Asia. The palaeobotanical values for Chinese localities are collected from the published literature (Xia et al., 2009; Jacques et al., 2011; Liu et al., 2011; Yao et al., 2011; Xing et al., 2012), and for Indian localities we use unpublished data (from T. Utescher, see Table S1 in the Supplement). The temperature values are estimated from either macrofossil (e.g., leaf, fruit and wood) or microfossil (e.g., pollen) assemblages using mainly the Coexistence Approach (CA) (Mosbrugger and Utescher, 1997; Utescher et al., 2014). The CA assumes that climatic tolerances of a fossil plant are equivalent to that of its nearest living relative (NLR), and estimates the climate conditions for a given fossil plant assemblage by overlapping the climatic tolerances of corresponding NLRs of each fossil taxon (i.e. the coexistence interval of NLRs) (Mosbrugger and Utescher, 1997). The CA can reconstruct various climate variables, but here we use only the mean annual temperature and coldest month temperature. Noted that the CA can only give an estimated interval, the width of which varies in dependence of climate requirements of NLRs involved. The real value can be at any position between the upper and lower ends of the interval. This introduces some complications when comparing the reconstructed temperature with the climate model or observation data. To overcome these issues, we use the Hagamann distance based on fuzzy logic (Guiot et al., 1999) to define the difference between the plant fossil reconstruction and the observation or model data. More detail on this method is described in the Supplement.

CPD
11, 63–93, 2015

For the mammal fossil reconstructions, we use published method (Liu et al., 2012) to estimate mean annual temperature and coldest quarter temperature based on the molar tooth crown properties of the mammal communities (See Table S2 in the Supplement). These properties are mean molar tooth crown height, i.e., hypsodonty and the mean longitudinal loph count of herbivore taxa found at a locality. All the Asian mammal fossil data are obtained from the NOW database (downloaded on 28 November 2012 from http://www.helsinki.fi/science/now/).

2.2 Climate model simulations

The Late Miocene climate simulations with a fully coupled global climate model ECHAM5/MPIOM (Micheels et al., 2011) and a regional climate model COSMO-CLM (Tang et al., 2011), are employed to demonstrate surface temperature and winter monsoon changes in the Late Miocene. They are referred to as GLMio and RLMio. The corresponding present-day control runs are referred to as GCTRL and RCTRL, respectively (Table 1). The global model simulations use T31 resolution ($3.75^\circ \times 3.75^\circ$) with 19 terrain-following vertical layers for its atmospheric model ECHAM5 and $3^\circ \times 3^\circ$ and 40 unevenly spaced vertical levels for its ocean circulation model MPIOM. The regional model runs are driven by the global model output, and cover the Asian monsoon area with a spatial resolution of $1^\circ \times 1^\circ$ on the rotated model grid and 20 vertical levels. To better represent the Late Miocene climate, the physical boundary conditions, such as orography, land–sea distribution and vegetation, were modified in GLMio and RLMio (see details in the Supplement). Particularly in Asia, the height of the northern Tibetan Plateau (TP) and the mountains north of it was greatly reduced (according to Zheng et al., 2006; Wang et al., 2008; Jolivet et al., 2007; Charreau et al., 2009), while the southern TP was kept close to present height in both experiments (according to Rowley et al., 2001; Spicer et al., 2003; Polissar et al., 2009) (Fig. 2). GLMio was integrated over 2600 years so that the model runs are in their dynamic equilibrium in terms of global mean temperature and sea ice volume. We use the last 110 year model integrations for analysis. Since our regional model requires only several months

CPD
11, 63–93, 2015

to spin up (Tang et al., 2011), RLMio was integrated for only 110 years, and the last 109 year results were used for analysis. It has been shown that both GLMio and RLMio can represent the Late Miocene Asian monsoon climate satisfyingly (Micheels et al., 2011; Tang et al., 2011, 2013a). But the high-resolution regional model can better depict small-scale orography and its influence on climate over the Asian monsoon region (Tang et al., 2011, 2013b). It is, therefore, expected to offer more precise insights into the winter monsoon and temperature changes in the Late Miocene than its driving global model.

To further assess the contribution of different factors to surface temperature and winter monsoon changes in the Late Miocene, an additional global and regional model experiment were performed (Table 1). In the global model experiment GLMioPD, all the boundary conditions are kept the same as GLMio, except that the orography in Asia are prescribed as present. It was initialised from the restart files of GLMio at 2500 year and was integrated for 100 years. We use the last 10 year results for analysis. In the regional model experiment RLMioPD, the model is driven by the output of GLMio but uses the present-day regional orography. It was integrated for 10 years and the last 9 year results were used for analysis. By comparing the climatologies of GLMioPD (RLMioPD) with that of GLMio (RLMio) and GCTRL (RCTRL), the influence of Late Miocene Asian orography and other boundary condition changes on the monsoon strength can be distinguished, respectively.

3 Results

The difference of mean annual (winter) temperature between the Late Miocene and the present as indicated by the proxy and model are displayed in Fig. 3. Both the plant and mammal fossil data reveal a generally higher-than-present annual temperature over the Asian continent in the Late Miocene (Fig. 3a and b), which is consistent with the warmer global conditions of this period (Pound et al., 2011). The increase of surface temperature is most pronounced in high-latitude regions and the TP, but is relatively

CPD
11, 63–93, 2015

small over the low-latitudes. In southern China and northern India, there are even plant and mammal fossil localities indicating lower temperature in the Late Miocene than at present (Fig. 3a and b), which is at odds with the warmer global climate in this period. Such decrease of mean annual temperature mostly results from the winter temperature changes. As shown in Fig. 3c and d, the coldest month (quarter) temperature derived from fossil data exhibit similar cooling as that of mean annual temperature in southern China and India, while the warmest month temperature does not (see Fig. 6).

Both our global and regional model runs capture the first-order feature of temperature changes in the Late Miocene, i.e., strong increase (weak increase or decrease) of temperature in the high-(low-)latitude Asia (Fig. 3). However, the decrease of temperature over southern China and northern India as indicated by proxy data is not observed in GLMio in both annual and winter temperature (Fig. 3a and c). RLMio also underestimates the drop of temperature in southern China and northern India, but displays a more pronounced decline of temperature (particularly in winter) over northern India and much smaller increase of temperature over southern China and the Indochina subcontinent than GLMio (Fig. 3b and d). It therefore yields a better agreement with the proxy data in these regions.

To understand the cooling of southern China and India shown in the proxy and the warm "biases" of GLMio and RLMio in these regions, temperature and the associated changes in sea level pressure and low-level wind in both the global and regional model experiments are shown in Fig. 4. It is indicated that the decrease of winter temperature in southern China and northern India can be linked to a strong winter monsoon primarily induced by the Late Miocene Asian orography (Fig. 4e and f). In particular, the lower height of the northern TP results in an increase of sea level pressure over the plateau but a decrease of sea level pressure to the north of the plateau. This guides a stronger low-level westerly wind through the north of the plateau, facilitating the winter monsoon wind and the decline of winter temperature in East Asia and India (Fig. 4e and f). Such an effect is further manifested by our regional mountain uplift experiments, in which the winter monsoon wind is strengthened by the absence of the northern and southeastern

CPD
11, 63–93, 2015

TP, causing winter temperature to drop considerably over China and India (see Fig. S1 in the Supplement).

In contrast to the effect of Late Miocene Asian orography, the other Late Miocene boundary conditions have little influence on the winter monsoon, and thus give rise to a general increase of winter temperature in the monsoon region representing warmer Late Miocene conditions (Fig. 4c and d). This warming effect is relatively strong in northern China (Fig. 4c and d). This counteracts the cooling effect of strong winter monsoon due to the Late Miocene Asian orography (Fig. 4e and f) and thus leads to an increase of temperature in northern China in both GLMio and RLMio (Fig. 4a and b). In comparison, the warming is relatively small in southern China and India (Fig. 4c and d). As a result, the cooling effect of strong winter monsoon (Fig. 4e and f) is better detected in these regions in GLMio and RLMio (Fig. 4a and b).

Fig. 5 illustrates the composite difference of winter surface temperature, sea level pressure and low-level wind between strong and weak winter monsoon years in our climate model runs. In the present-day control runs, both the global and regional models correctly represent the close relation among winter monsoon wind, Siberian High/Aleutian Low and surface temperature over East China and India as that shown in the Reanalysis Data (cf., Figs. 5a and b and 1). In comparison, both models simulate a much weaker decrease of surface temperature over the continent during the strong winter monsoon years in their Late Miocene runs (Fig. 5c and d). The strengthening of the Siberian High during the strong winter monsoon years is also much reduced in the Late Miocene runs, even though the deepening of the Aleutian Low over the North Pacific persists. These differences between the Late Miocene and present-day runs imply that the modern-like winter monsoon system with strong association of Siberian High and surface temperature changes on the inter-annual scale may not have established in the Late Miocene.

CPD
11, 63–93, 2015

Strong winter monsoon causes Miocene cooling

H. Tang et al.

Title Page
Abstract Introduction
Conclusions References
Tables Figures
◄ ►
Back Close
Full Screen / Esc
Printer-friendly Version
Interactive Discussion

4 Discussion

4.1 Cooler winter in the Late Miocene

Cooler winter in the Miocene and earlier periods has been recently noticed in several plant fossil localities from southern China (Quan et al., 2012; Zhang et al., 2012). Our compilation of the Late Miocene plant and mammal fossil reconstructions in Asia reveals some heterogeneity between localities (Fig. 3 and Tables S1 and S2) due to either uncertainties of the reconstruction methods or to unknown orography details of different localities in the Late Miocene. But all for that, there is a clear indication of overall cooler conditions in southern China and northern India in the Late Miocene in contrast to northern China where estimates show uniformly warmer-than-present conditions (Fig. 3).

In southern China, the evidence for cooler Late Miocene winter temperature mostly comes from reconstructions based on plant fossils using the Coexistence Approach (CA). The Climate Leaf Analysis Multivariate Program (CLAMP) and Leaf Margin Analysis have also been used to reconstruct temperature in some plant fossil localities from southwest China, both supporting lower-than-present winter temperature in the Late Miocene (see Table S1) (Xing et al., 2012). This gives us confidence in the Late Miocene temperature reconstructions for this region. The plant fossil records are relatively sparse in the Indian and Indochina subcontinent, but 3 out of the 4 available localities indicate cooler-than-present annual or winter temperature. In particular, we reconstruct temperature of the locality in Nepal for three different periods of the Late Miocene based on pollen data from Hoorn et al. (2000) (see Sural Khola in Fig. 6a). The earlier periods (i.e., 11.5–8 and 8–6 Ma) display cooler than present temperature while the later period (6–5 Ma) shows marked increase in temperature, particularly in winter. This indicates that the cooler-than-present surface temperature may have mainly existed in the earlier Late Miocene (i.e., before 6 Ma).

Using molar tooth crown properties (i.e., hypsodonty and loph count) of fossil mammals to reconstruct surface temperature is a novel method recently developed by Liu et al. (2012). It is based on the observation that in today's mammal faunas, mammalian herbivore assemblages with higher mean number of longitudinal cutting edges (loph score) and low mean molar crown height (hypsodonty score) are associated with colder environments and thus indicative of lower temperature, and vice versa. The linear regression model using these two properties as predictors is fairly robust in predicting the global pattern of temperature at present day (Liu et al., 2012). In particular, the coldest quarter temperature (i.e, winter temperature) is best predicted by these dental traits (Liu et al., 2012), a circumstance attributable to the fact that these dental traits are more linked to the length and frequency of harsh intervals, when nothing but mechanically demanding and nutrient-poor food is available, than to the average properties of foods available in average years (Fortelius et al., 2014). Applying the same model to the Late Miocene fossil localities also reveals a cooler-than-present surface temperature in several localities in the Indian and Indochina Subcontinent (Fig. 3b and d). This corroborates the cooler condition of these regions in the Late Miocene. We note that the locality in central India may have too low temperature estimate, due to short species list (only two taxa are recorded, both of which have low hypsodonty but high loph count, see Eronen et al. 2012, for further discussion on the short list anomaly). Except this locality, all the other localities showing cooler-than-present temperature have long species list, offering a good representation of the mammal assemblage and thus reliable temperature estimate. The reason for the cooler temperature estimates in these localities is mainly the absence of species with low loph count, such as primates.

Compared to the plant and mammal proxies, our Late Miocene climate model runs show consistently warm "biases" in southern China and India. Nevertheless, the sensitivity experiments reveal that the cooler-than-present winter temperature in the Late Miocene can be physically plausible and explained by the strong winter monsoon due to the Late Miocene Asian orography changes, i.e. the lower elevation of the northern TP and the mountains north of it. As shown in Fig. 6, both global and regional Late Miocene model runs (GLMio and RLMio) fail to reproduce the decrease of annual or winter temperature compared to present day as showed in the selected fossil

CPD
11, 63–93, 2015

localities from southern China and India. But considering only the effect of the Late Miocene orography changes (RLMio-RLMioPD), the regional model is able to produce the decrease of annual or winter temperature in all these fossil localities, even though the magnitude is still smaller than that indicated by the proxies. In all the selected plant fossil localities, temperature change in summer is more positive than in winter (Fig. 6a). This is also well captured by the effect of the Late Miocene orography changes (RLMio-RLMioPD).

We note that the cooling effect of strong winter monsoon can be further enhanced by its interaction with ocean circulation. A prominent shoaling of the thermocline over northern South China Sea has been reported to occur in 8–7 Ma as a result of a strong winter monsoon leading to enhanced offshore flow (Zheng et al., 2004). This may have given rise to a further decrease of surface temperature in the surrounding area, and explains why the drop of winter temperature is most evident in the fossil localities along the coast of southern China (Fig. 3c). In our regional Late Miocene model run (RLMio), the lack of decrease of winter temperature in southern China compared to the proxies (Fig. 3d) can be related to the prescribed sea surface temperature in the model that cannot represent the influence of winter monsoon on ocean water mixing. In contrast, our fully coupled global model depicts this interaction, and thus displays a more significant cooling over the East China Sea in response to the enhanced winter monsoon (cf., Figs. 4a and e and 4b and f).

In general, our regional model perform better in depicting the winter cooling over southern China and India in the Late Miocene (Fig. 3 and 6). Although our global model also simulates stronger winter monsoon in the Late Miocene, it fails to capture any cooling in the continental Asia (Fig. 4a). This can be ascribed to either too overwhelming global warming effect (Fig. 4c) or too weak cold air advection with the winter monsoon (Fig. 4e). The discrepancies between model and proxy in depicting the winter cooling in southern China and India in the Late Miocene highlight the importance of more temperature reconstructions over India and southern China using different proxies such as clumped isotopes (e.g., Suarez et al., 2011) and biomarkers (e.g., Peterse et al., 2014) to test this pattern. On a model perspective, more sensitivity experiments using the fully coupled models with different Late Miocene boundary conditions, such as vegetation and surface elevation, are required to better understand the source of the warm “biases” in the model.

4.2 Strong winter monsoon wind in the Late Miocene

The winter cooling as manifested in our proxy data together with our modelling results points to a strong winter monsoon in the Late Miocene. This is in contrast to previous studies which suggest a weaker-than-present winter monsoon in this period (Guo et al., 2002; Jia et al., 2003; Fan et al., 2006; Wan et al., 2007; D. H. Sun et al., 2008; Jiang and Ding, 2010). We note that most of these studies use accumulation rate of aeolian deposit to infer the winter monsoon strength. This proxy, however, is questionable, because it is not only modulated by the winter monsoon strength, but also influenced by the conditions (e.g., vegetation and wind speed) in the dust source and capture regions (Yue et al., 2009; Shi et al., 2011). In addition, dust storms occur more frequently in spring than in winter (Molnar et al., 2010), indicating dust accumulation rate may not be a direct winter monsoon proxy. Instead, using quartz grain size (or coarse particle size) fraction of aeolian deposit as a proxy for winter monsoon strength, Vandenberghe et al. (2004) and Y. B. Sun et al. (2010) claimed a relatively strong winter monsoon in the Late Miocene. A winter monsoon dominated climate over the western Loess Plateau before 6 Ma is also reported by Li et al. (2008, 2014), who use cold-philous species of fossil snails as an indicator for the winter monsoon strength. A recent model study using the ensemble of Mid-Pliocene global simulations also revealed a stronger-than-present winter monsoon wind in southern China and India (Zhang et al., 2013).This further supports the existence of a strong winter monsoon in the pre-Quaternary periods when the global climate was generally warmer.

Our model results suggest that the Late Miocene Asian orography, i.e., the lower elevation of northern TP and the mountains north of it, can be responsible for the strong winter monsoon in the Late Miocene (Fig. 4e and f). This is distinct from the conventional modelled effect of the whole TP, which states that the growth and uplift of the entire TP strengthens the Siberian High and the winter monsoon wind in East Asia, and vice versa (Kutzbach et al., 1993; An et al., 2001; Liu and Yin, 2002). We notice that the low Late Miocene Asian orography indeed weakens the Siberian High over northern Eurasia (Fig. 4e and f), which agrees with previous studies (Kutzbach et al., 1993; An et al., 2001; Liu and Yin, 2002). But the pressure over the Japan Sea and North Pacific is also weakened (Fig. 4e). As a result, the pressure gradient between the Siberian High and the Aleutian Low is not strongly modified (compare monsoon index SH of G(R)LMio with that of G(R)LMioPD in Table 2). Meanwhile, we see a strong positive pressure anomaly over the TP due to the reduced height of the northern TP (Fig. 4e and f). This enhances the pressure gradient between the TP and the northern Eurasia, and thus intensifies the westerly wind through the north of the plateau that eventually causes a strong winter monsoon wind in East Asia.

The Late Miocene orography, i.e., the lower elevation of northern TP and the mountains north of it, also promotes the upper tropospheric westerly jet stream over the northern TP, northern China and southern Japan and weakens the westerly flow to the north of it (Fig. 7e and f). This is similar to that observed between strong and weak winter monsoon years at present (Fig. 1b). According to Jhun and Lee (2004), such dipole changes in the upper-level westerly wind speed indicate anomalous cyclonic vorticity to the north of the jet stream over East Asia (compare monsoon index JS of G(R)LMio with that of G(R)LMioPD in Table 2) that can strengthen the mid-tropospheric monsoon trough and thus the low-level winter monsoon wind. The dominance of the westerly flow in maintaining the winter monsoon in the Late Miocene as suggested by our model results is concordant with the studies by Ding et al. (1999), Sun (2004) and Vandenberghe et al. (2004), which emphasize the importance of westerly flow for dust transport in the Late Miocene. It also agrees with geochemical evidence implying a much higher contribution of dust materials to the Loess Plateau from its west (i.e., Qilian Mountains) than from its north (i.e., Gobi Altay Mountains) in the Late Miocene (Chen and Li, 2013).

CPD
11, 63–93, 2015

Compared to the effect of the Late Miocene Asian orography, the other Late Miocene boundary conditions seem to have slightly opposite effect on the upper-level westerly jet stream (Fig. 7c and d and Table 2). They also reduce the pressure gradient between Siberian High and Aleutian Low (compare monsoon index SH of G(R)LMioPD with that of G(R)CTRL in Table 2), and thus favour a slightly weakened winter monsoon wind in East Asia (Fig. 4c). We note that the response of upper-level westerly flow to the Late Miocene Asian orography is much weaker in our regional model experiment than in the global model (cf., Fig. 7e and f), even though the patterns are similar. This can be ascribed to the strong control of global forcing on the upper level circulation in winter in the regional model. Accordingly, global model should be more sensitive than the regional model in depicting the upper-level winter monsoon response to the Asian orography changes.

Recent model studies have revealed that different parts of the Asian orography have distinct influence on the Siberian High and the westerly jet stream and therefore the winter monsoon (Shi et al., 2014; Zhang et al., 2014). Zhang et al. (2014) showed that the presence of the middle TP can enhance the Siberian High but reduce the winter monsoon wind in East China (Fig. 10a in their paper), which is consistent with our modelled effect of the Late Miocene Asian orography (Fig. 4e). However, they showed that the presence of the northern TP can enhance the northerly wind in East China, which is contradictory to our model results. Also seemingly contrary to our results, Shi et al. (2014) reported that the presence of the mountains north of the TP (i.e., Tianshan Mountains and Mongolian Plateau) is essential for the enhancement of the westerly jet over Japan. The Late Miocene orography used in our model experiments include both the lower-than-present northern TP and the mountains north of it. The combined effect of these orography changes might be different from their individual effects (Tang et al., 2013b). More modelling studies are needed to better understand the individual as well as the combined effect of different regional orography in Asia on the westerly jet and Siberian High that together determine the winter monsoon strength.

4.3 The establishment of modern winter monsoon system

A previous study has suggested that the modern-like Siberian High driven winter monsoon system might have existed as early as in the Late Oligocene (Y. B. Sun et al., 2010). This, however, is not supported by our model results. The winter monsoon in the Late Miocene has a marked westerly wind component, and the Siberian High is still weak due to the warmer high-latitudes and the low Asian orography (Fig. 4a and b). As a result, we do not observe a strong association of Siberian High and winter temperature changes with the strength of winter monsoon wind on inter-annual scale in the Late Miocene (Fig. 5c and d) as that at present (Fig. 5a and b). Further uplift of the northern TP (Zheng et al., 2006; Wang et al., 2008) and the Gobi Altay Mountains (Jolivet et al., 2007) (which weakens the low-level westerly flow to the north of the TP), and the cooling of the Northern Hemisphere (which strengthens the Siberian High), might be essential for the shift from a westerly driven to a Siberian High driven winter monsoon regime, and the emergence of the modern-like winter monsoon system.

5 Conclusions

Modern observations reveal a close association between surface temperature and the Asian winter monsoon strength. In this study, we examine this relationship in the Late Miocene by analysing the temperature reconstructions from plant and mammal fossil records and the climate model results. We find that a strong winter monsoon wind might have existed in the Late Miocene owing to the lower elevation of the northern Tibetan Plateau and the mountains north of it. This can lead to a cooler-than-present temperature (particularly in winter) in southern China and northern India, which is opposite to the warmer global conditions in this period. The Late Miocene winter monsoon had a marked westerly component, while the Siberian High was still weak due to warmer global climate and the lower Asian orography. As a result, the modern-like interannual variation of the winter monsoon with a strong association with the Siberian High and the surface temperature changes in the monsoon region may not have been fully established in the Late Miocene. Both the global and regional models are useful tools to study the winter monsoon changes in geological periods. While the global model is more sensitive in depicting the response of sea level pressure and upper-level circulation to Asian orography changes, the high-resolution regional model may better capture the surface temperature changes in accordance to the winter monsoon strength.

The Supplement related to this article is available online at doi:10.5194/cpd-11-63-2015-supplement.

Acknowledgements. This work was supported by the Academy of Finland Research Fellow Projects No. 257858 and No. 264935 (A. Kaakinen and H. Tang), and EU Marie Curie Fellowship (J. T. Eronen). We acknowledge the model support of the CLM community and the technical support from Center for Scientific Computing (CSC) in Espoo (Finland). We also would like to thank Arne Micheels for providing the global model data (GCTRL and GLMio), and Kai Puolamäki for the help with mammal fossil reconstruction. This study is a contribution to NECLIME (Neogene Climate Evolution in Eurasia), and iCCB (integrative Climate Change Biology a program under IUBS).

References

An, Z. S., Kutzbach, J. E., Prell, W. L., and Porter, S. C.: Evolution of Asian monsoons and phased uplift of the Himalayan Tibetan plateau since Late Miocene times, Nature, 411, 62–66, 2001. 65, 75

Charreau, J., Chen, Y., Gilder, S., Barrier, L., Dominguez, S., Augier, R., Sen, S., Avouac, J. P., Gallaud, A., Graveleau, F., and Wang, Q. C.: Neogene uplift of the Tian Shan Mountains observed in the magnetic record of the Jingou River section (northwest China), Tectonics, 28, TC2008, doi:10.1029/2007TC002137, 2009. 67

Chen, Z. and Li, G.: Evolving sources of eolian detritus on the Chinese Loess Plateau since early Miocene: tectonic and climatic controls, Earth Planet. Sc. Lett., 371–372, 220–225, 2013. 75

Ding, Z. L., Xiong, S. F., Sun, J. M., Yang, S. L., Gu, Z. Y., and Liu, T. S.: Pedostratigraphy and paleomagnetism of a similar to 7.0 Ma eolian loess-red clay sequence at Lingtai, Loess Plateau, north-central China and the implications for paleomonsoon evolution, Palaeogeogr. Palaeocl., 152, 49–66, 1999. 75

Eronen, J. T., Fortelius, M., Micheels, A., Portmann, F., Puolamäki, K., and Janis, C. M.: Neogene aridification of the Northern Hemisphere, Geology, 40, 823–826, 2012. 72

Fan, M. J., Song, C. H., Dettman, D. L., Fang, X. M., and Xu, X. H.: Intensification of the Asian winter monsoon after 7.4 Ma: grain-size evidence from the Linxia basin, northeastern Tibetan Plateau, 13.1 Ma to 4.3 Ma, Earth Planet. Sc. Lett., 248, 186–197, 2006. 74

Fortelius, M., Eronen, J., Jernvall, J., Liu, L. P., Pushkina, D., Rinne, J., Tesakov, A., Vislobokova, I., Zhang, Z. Q., and Zhou, L. P.: Fossil mammals resolve regional patterns of Eurasian climate change over 20 million years, Evol. Ecol. Res., 4, 1005–1016, 2002. 65

Fortelius, M., Eronen, J. T., Kaya, F., Tang, H., Raia, P., and Puolamäki, K.: Evolution of Neogene mammals in Eurasia: environmental forcing and biotic interactions, Annu. Rev. Earth Pl. Sc., 42, 579–604, 2014. 72

Guiot, J., Boreux, J. J., Braconnot, P., and Torre, F.: Data-model comparison using fuzzy logic in paleoclimatology, Clim. Dynam., 15, 569–581, 1999. 66

Guo, Z. T., Ruddiman, W. F., Hao, Q. Z., Wu, H. B., Qiao, Y. S., Zhu, R. X., Peng, S. Z., Wei, J. J., Yuan, B. Y., and Liu, T. S.: Onset of Asian desertification by 22 Myr ago inferred from loess deposits in China, Nature, 416, 159–163, 2002. 65, 74

Hoorn, C., Ohja, T., and Quade, J.: Palynological evidence for vegetation development and climatic change in the Sub-Himalayan Zone (Neogene, Central Nepal), Palaeogeogr. Palaeocl., 163, 133–161, 2000. 71

Jacques, F. M. B., Guo, S.-X., Su, T., Xing, Y.-W., Huang, Y.-J., Liu, Y.-S., Ferguson, D. K., and Zhou, Z.-K.: Quantitative reconstruction of the Late Miocene monsoon climates of southwest China: a case study of the Lincang flora from Yunnan Province, Palaeogeogr. Palaeocl., 304, 318–327, 2011. 66

Jacques, F. M. B., Shi, G., and Wang, W. M.: Neogene zonal vegetation of China and the evolution of the winter monsoon, B. Geosci., 88, 175–193, 2013. 65

CPD
11, 63–93, 2015

Jhun, J. G. and Lee, E. J.: A new East Asian winter monsoon index and associated characteristics of the winter monsoon, J. Climate, 17, 711–726, 2004. 75, 86

Jia, G. D., Peng, P. A., Zhao, Q. H., and Jian, Z. M.: Changes in terrestrial ecosystem since 30 Ma in East Asia: stable isotope evidence from black carbon in the South China Sea, Geology, 31, 1093–1096, 2003. 65, 74

Jiang, H. C. and Ding, Z. L.: Eolian grain-size signature of the Sikouzi lacustrine sediments (Chinese Loess Plateau): implications for Neogene evolution of the East Asian winter monsoon, Geol. Soc. Am. Bull., 122, 843–854, 2010. 65, 74

Jolivet, M., Ritz, J. F., Vassallo, R., Larroque, C., Braucher, R., Todbileg, M., Chauvet, A., Sue, C., Arnaud, N., De Vicente, R., Arzhanikova, A., and Arzhanikov, S.: Mongolian summits: an uplifted, flat, old but still preserved erosion surface, Geology, 35, 871–874, 2007. 67, 77

Kalnay, E., Kanamitsu, M., Kistler, R., Collins, W., Deaven, D., Gandin, L., Iredell, M., Saha, S., White, G., Woollen, J., Zhu, Y., Chelliah, M., Ebisuzaki, W., Higgins, W., Janowiak, J., Mo, K. C., Ropelewski, C., Wang, J., Leetmaa, A., Reynolds, R., Jenne, R., and Joseph, D.: The NCEP/NCAR 40-year reanalysis project, B. Am. Meteorol. Soc., 77, 437–471, 1996. 87

Kutzbach, J. E., Prell, W. L., and Ruddiman, W. F.: Sensitivity of Eurasian climate to surface uplift of the Tibetan Plateau, J. Geol., 101, 177–190, 1993. 65, 75

Li, F., Wu, N., Rousseau, D.-D., Dong, Y., Zhang, D., and Pei, Y.: Late Miocene? Pliocene paleoclimatic evolution documented by terrestrial mollusk populations in the western Chinese Loess Plateau, PLoS ONE, 9, e95754, doi:10.1371/journal.pone.0095754, 2014. 65, 74

Li, F. J., Rousseau, D. D., Wu, N. Q., Hao, Q. Z., and Pei, Y. P.: Late Neogene evolution of the East Asian monsoon revealed by terrestrial mollusk record in Western Chinese Loess Plateau: from winter to summer dominated sub-regime, Earth Planet. Sc. Lett., 274, 439–447, 2008. 65, 74

Licht, A., van Cappelle, M., Abels, H. A., Ladant, J. B., Trabucho-Alexandre, J., France-Lanord, C., Donnadieu, Y., Vandenberghe, J., Rigaudier, T., Lecuyer, C., Terry Jr., D., Adriaens, R., Boura, A., Guo, Z., Soe, A. N., Quade, J., Dupont-Nivet, G., and Jaeger, J. J.: Asian monsoons in a late Eocene greenhouse world, Nature, 513, 501–506, 2014. 65

Liu, L., Puolamaki, K., Eronen, J. T., Ataabadi, M. M., Hernesniemi, E., and Fortelius, M.: Dental functional traits of mammals resolve productivity in terrestrial ecosystems past and present, P. Roy. Soc. B-Biol. Sci., 279, 2793–2799, 2012. 67, 71, 72

CPD
11, 63–93, 2015

Liu, X. D. and Yin, Z. Y.: Sensitivity of East Asian monsoon climate to the uplift of the Tibetan Plateau, Palaeogeogr. Palaeocl., 183, 223–245, 2002. 65, 75

Liu, Y. S., Utescher, T., Zhou, Z. K., and Sun, B. N.: The evolution of Miocene climates in North China: preliminary results of quantitative reconstructions from plant fossil records, Palaeogeogr. Palaeocl., 304, 308–317, 2011. 66

Lu, H. and Guo, Z.: Evolution of the monsoon and dry climate in East Asia during late Cenozoic: a review, Science China Earth Sciences, 57, 70–79, 2014. 65

Micheels, A., Bruch, A. A., Eronen, J. T., Fortelius, M., Harzhauser, M., Utescher, T., and Mosbrugger, V.: Analysis of heat transport mechanisms from a Late Miocene model experiment with a fully-coupled atmosphere–ocean general circulation model, Palaeogeogr. Palaeocl., 304, 337–350, 2011. 67, 68

Molnar, P., Boos, W. R., and Battisti, D. S.: Orographic controls on climate and paleoclimate of Asia: thermal and mechanical roles for the Tibetan Plateau, Annu. Rev. Earth Pl. Sc., 38, 77–102, 2010. 65, 74

Mosbrugger, V. and Utescher, T.: The coexistence approach – a method for quantitative reconstructions of Tertiary terrestrial palaeoclimate data using plant fossils, Palaeogeogr. Palaeocl., 134, 61–86, 1997. 66

Peterse, F., Martinez-Garcia, A., Zhou, B., Beets, C. J., Prins, M. A., Zheng, H., and Eglinton, T. I.: Molecular records of continental air temperature and monsoon precipitation variability in East Asia spanning the past 130,000 years, Quaternary Sci. Rev., 83, 76–82, 2014. 73

Polissar, P. J., Freeman, K. H., Rowley, D. B., McInerney, F. A., and Currie, B. S.: Paleoaltimetry of the Tibetan Plateau from D/H ratios of lipid biomarkers, Earth Planet. Sc. Lett., 287, 64–76, 2009. 67

Pound, M. J., Haywood, A. M., Salzmann, U., Riding, J. B., Lunt, D. J., and Hunter, S. J.: A Tortonian (Late Miocene, 11.61–7.25 Ma) global vegetation reconstruction, Palaeogeogr. Palaeocl., 300, 29–45, 2011. 68

Quan, C., Liu, Y.-S., and Utescher, T.: Eocene monsoon prevalence over China: A paleobotanical perspective, Palaeogeogr. Palaeocl., 365–366, 302–311, 2012. 65, 71

Rowley, D. B., Pierrehumbert, R. T., and Currie, B. S.: A new approach to stable isotope-based paleoaltimetry: implications for paleoaltimetry and paleohypsometry of the High Himalaya since the Late Miocene, Earth Planet. Sc. Lett., 188, 253–268, 2001. 67

Sakai, K. and Kawamura, R.: Remote response of the East Asian winter monsoon to tropical forcing related to El Niño–Southern Oscillation, J. Geophys. Res.-Atmos., 114, D06105, doi:10.1029/2008JD010824, 2009. 86

Shi, Z., Liu, X., An, Z., Yi, B., Yang, P., and Mahowald, N.: Simulated variations of eolian dust from inner Asian deserts at the mid-Pliocene, last glacial maximum, and present day: contributions from the regional tectonic uplift and global climate change, Clim. Dynam., 37, 2289–2301, 2011. 74

Shi, Z., Liu, X., Liu, Y., Sha, Y., and Xu, T.: Impact of Mongolian Plateau versus Tibetan Plateau on the westerly jet over North Pacific Ocean, Clim. Dynam., 1–10, doi:10.1007/s00382-014-2217-2, 2014. 76

Spicer, R. A., Harris, N. B. W., Widdowson, M., Herman, A. B., Guo, S. X., Valdes, P. J., Wolfe, J. A., and Kelley, S. P.: Constant elevation of southern Tibet over the past 15 million years, Nature, 421, 622–624, 2003. 67

Suarez, M. B., Passey, B. H., and Kaakinen, A.: Paleosol carbonate multiple isotopologue signature of active East Asian summer monsoons during the late Miocene and Pliocene, Geology, 39, 1151–1154, 2011. 73

Sun, D. H.: Monsoon and westerly circulation changes recorded in the late Cenozoic aeolian sequences of Northern China, Global Planet. Change, 41, 63–80, 2004. 75

Sun, D. H., Su, R. X., Bloemendal, J., and Lu, H. Y.: Grain-size and accumulation rate records from Late Cenozoic aeolian sequences in northern China: implications for variations in the East Asian winter monsoon and westerly atmospheric circulation, Palaeogeogr. Palaeocl., 264, 39–53, 2008. 74

Sun, J. M., Ye, J., Wu, W. Y., Ni, X. J., Bi, S. D., Zhang, Z. Q., Liu, W. M., and Meng, J.: Late Oligocene-Miocene mid-latitude aridification and wind patterns in the Asian interior, Geology, 38, 515–518, 2010. 77

Sun, Y. B., An, Z. S., and Clemens, S. C.: Non-stationary response of Plio-Pleistocene East Asian winter monsoon variation to ice volume forcing, Geological Society, London, Special Publications, 342, 79–86, 2010. 74

Tang, H., Micheels, A., Eronen, J., and Fortelius, M.: Regional climate model experiments to investigate the Asian monsoon in the Late Miocene, Clim. Past, 7, 847–868, doi:10.5194/cp-7-847-2011, 2011. 65, 67, 68

Tang, H., Eronen, J. T., Micheels, A., and Ahrens, B.: Strong interannual variation of the Indian summer monsoon in the Late Miocene, Clim. Dynam., 41, 135–153, 2013a. 68

Tang, H., Micheels, A., Eronen, J. T., Ahrens, B., and Fortelius, M.: Asynchronous responses of East Asian and Indian summer monsoons to mountain uplift shown by regional climate modelling experiments, Clim. Dynam., 40, 1531–1549, 2013b. 68, 76

Utescher, T., Bruch, A. A., Erdei, B., François, L., Ivanov, D., Jacques, F. M. B., Kern, A. K., Liu, Y. S., Mosbrugger, V., and Spicer, R. A.: The coexistence approach – theoretical background and practical considerations of using plant fossils for climate quantification, Palaeogeogr. Palaeocl., 410, 58–73, 2014. 66

Vandenberghe, J., Lu, H., Sun, D., van Huissteden, J., and Konert, M.: The late Miocene and Pliocene climate in East Asia as recorded by grain size and magnetic susceptibility of the Red Clay deposits (Chinese Loess Plateau), Palaeogeogr. Palaeocl., 204, 239–255, 2004. 65, 74, 75

Wan, S. M., Li, A. C., Clift, P. D., and Stuut, J. B. W.: Development of the East Asian monsoon: Mineralogical and sedimentologic records in the northern South China Sea since 20 Ma, Palaeogeogr. Palaeocl., 254, 561–582, 2007. 65, 74

Wang, P. X., Clemens, S., Beaufort, L., Braconnot, P., Ganssen, G., Jian, Z. M., Kershaw, P., and Sarnthein, M.: Evolution and variability of the Asian monsoon system: state of the art and outstanding issues, Quaternary Sci. Rev., 24, 595–629, 2005. 65

Wang, Y., Wang, X. M., Xu, Y. F., Zhang, C. F., Li, Q., Tseng, Z. J., Takeuchi, G., and Deng, T.: Stable isotopes in fossil mammals, fish and shells from Kunlun Pass Basin, Tibetan Plateau: Paleo-climatic and paleo-elevation implications, Earth Planet. Sc. Lett., 270, 73–85, 2008. 67, 77

Xia, K., Su, T., Liu, Y. S., Xing, Y. W., Jacques, F. M. B., and Zhou, Z. K.: Quantitative climate reconstructions of the late Miocene Xiaolongtan megaflora from Yunnan, southwest China, Palaeogeogr. Palaeocl., 276, 80–86, 2009. 66

Xing, Y., Utescher, T., Jacques, F. M. B., Su, T., Liu, Y., Huang, Y., and Zhou, Z.: Paleoclimatic estimation reveals a weak winter monsoon in southwestern China during the late Miocene: evidence from plant macrofossils, Palaeogeogr. Palaeocl., 358–360, 19–26, 2012. 66, 71

Yao, Y.-F., Bruch, A. A., Mosbrugger, V., and Li, C.-S.: Quantitative reconstruction of Miocene climate patterns and evolution in Southern China based on plant fossils, Palaeogeogr. Palaeocl., 304, 291–307, 2011. 66

Yue, X., Wang, H., Wang, Z., and Fan, K.: Simulation of dust aerosol radiative feedback using the Global Transport Model of Dust: 1. Dust cycle and validation, J. Geophys. Res.-Atmos., 114, D10202, doi:10.1029/2008jd010995, 2009. 74

Zhang, Q.-Q., Ferguson, D. K., Mosbrugger, V., Wang, Y.-F., and Li, C.-S.: Vegetation and climatic changes of SW China in response to the uplift of Tibetan Plateau, Palaeogeogr. Palaeocl., 363–364, 23–36, 2012. 65, 71

Zhang, R., Yan, Q., Zhang, Z. S., Jiang, D., Otto-Bliesner, B. L., Haywood, A. M., Hill, D. J., Dolan, A. M., Stepanek, C., Lohmann, G., Contoux, C., Bragg, F., Chan, W.-L., Chandler, M. A., Jost, A., Kamae, Y., Abe-Ouchi, A., Ramstein, G., Rosenbloom, N. A., Sohl, L., and Ueda, H.: Mid-Pliocene East Asian monsoon climate simulated in the PlioMIP, Clim. Past, 9, 2085–2099, doi:10.5194/cp-9-2085-2013, 2013. 74

Zhang, R., Jiang, D., Zhang, Z., and Yu, E.: The impact of regional uplift of the Tibetan Plateau on the Asian monsoon climate, Palaeogeogr. Palaeocl., 47, 137–150, 2015. 65, 76

Zheng, D. W., Zhang, P. Z., Wan, J. L., Yuan, D. Y., Li, C. Y., Yin, G. M., Zhang, G. L., Wang, Z. C., Min, W., and Chen, J.: Rapid exhumation at similar to 8 Ma on the Liupan Shan thrust fault from apatite fission-track thermochronology: implications for growth of the northeastern Tibetan Plateau margin, Earth Planet. Sc. Lett., 248, 198–208, 2006. 67, 77

Zheng, H., Powell, C. M., Rea, D. K., Wang, J., and Wang, P.: Late Miocene and mid-Pliocene enhancement of the East Asian monsoon as viewed from the land and sea, Global Planet. Change, 41, 147–155, 2004. 73

Table 1. List of model experiments in this study.

Exp. ID	Description
GCTRL	Present-day global model run
GLMio	Late Miocene global model run
GLMioPD	Same as GLMio except that the present-day orography in Asia (see box in Fig. 2a) is used.
RCTRL	Present-day regional model run
RLMio	Late Miocene regiona model run
RLMioPD	Regional model run using Late Miocene global forcing (i.e., GLMio) but present-day regional orography.

CPD
11, 63–93, 2015

Strong winter monsoon causes Miocene cooling

H. Tang et al.

Table 2. Winter monsoon indices in different global and regional model experiments. The Effect of the Late Miocene Asian orography changes and other Late Miocene boundary conditions on the winter monsoon can be deduced by comparing G(R)LMio with G(R)LMioPD and comparing G(R)LMioPD with G(R)CTRL. SH (hPa) denotes mean sea level pressure difference between the locations in Russia (106.1° E, 52.9° N) and Japan (145.0° E, 43.6° N) in winter (Sakai and Kawamura, 2009). JS ($m\,s^{-1}$) denotes 300 hPa zonal wind shear between 110–140° E, 27.5–37.5° N and 80–120° E, 50–60° N in winter (Jhun and Lee, 2004).

	GCTRL	GLMio	GLMioPD	RCTRL	RLMio	RLMioPD
SH	26.08	20.96	20.66	20.57	15.19	16.19
JS	33.40	35.71	28.98	37.85	38.06	37.04

CPD
11, 63–93, 2015

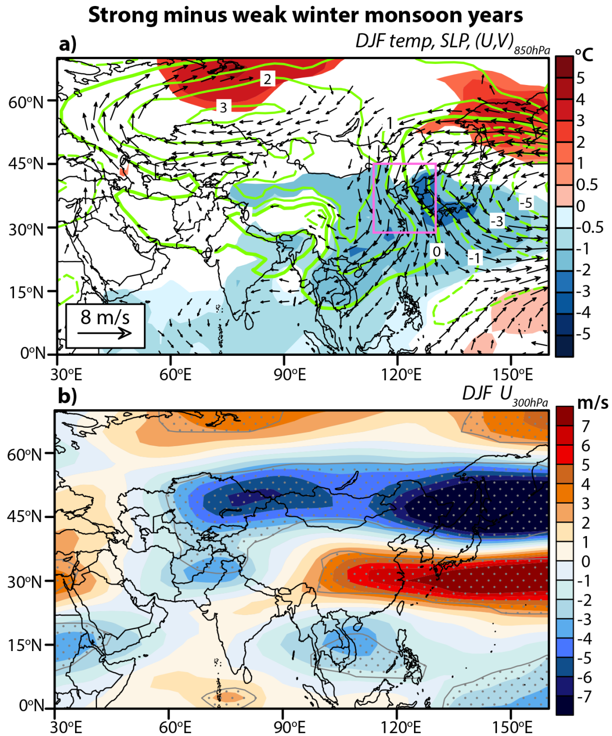

Figure 1. Composite difference of **(a)** winter temperature (°C) (shaded), 850 hPa wind (m s^{-1}) (vector) and sea level pressure (hPa) (contour) and **(b)** 300 hPa zonal wind between the strong and weak winter monsoon years based on NCEP/NCAR reanalysis (1948–2011) (Kalnay et al., 1996). Colour shading (black vector) in **(a)** denotes temperature (wind) differences significant with a Student's t test ($p < 0.05$). Positive (negative) sea level pressure differences are denoted by solid (dashed) contour. The strong (weak) winter monsoon years are defined as the years when the northerly wind strength over 110–130° E, 25–45° N (purple box in **a**) is higher (lower) than the multi-year average with one SD.

CPD
11, 63–93, 2015

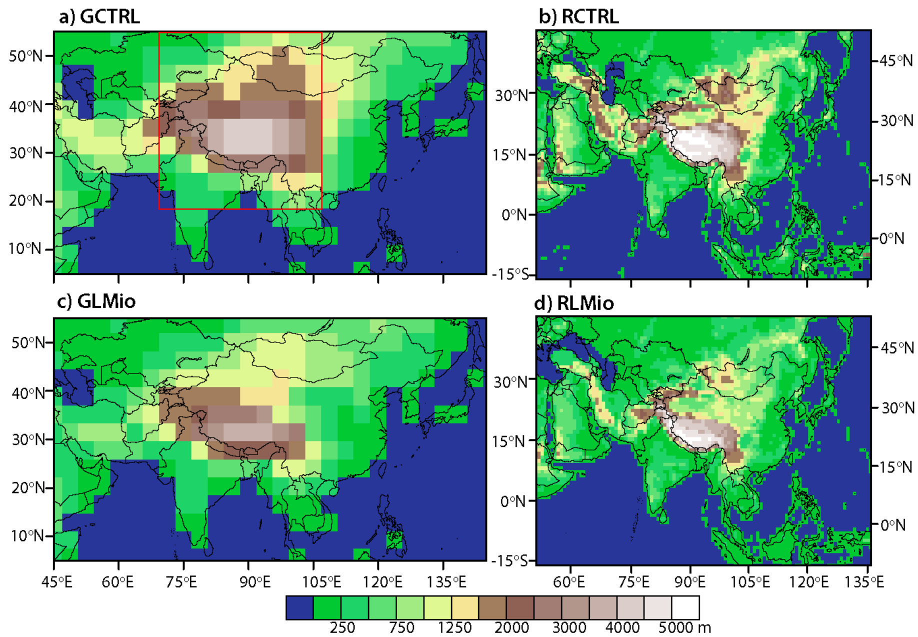

Figure 2. Surface elevation in global model present-day control run (GCTRL) **(a)** and Late Miocene run (GLMio) **(c)**, and in regional model present-day control run (RCTRL) **(b)** and Late Miocene run (RLMio) **(d)**. The red box in **(a)** denotes the region where the present-day orography is prescribed in the global model experiment GLMioPD (see Table 1).

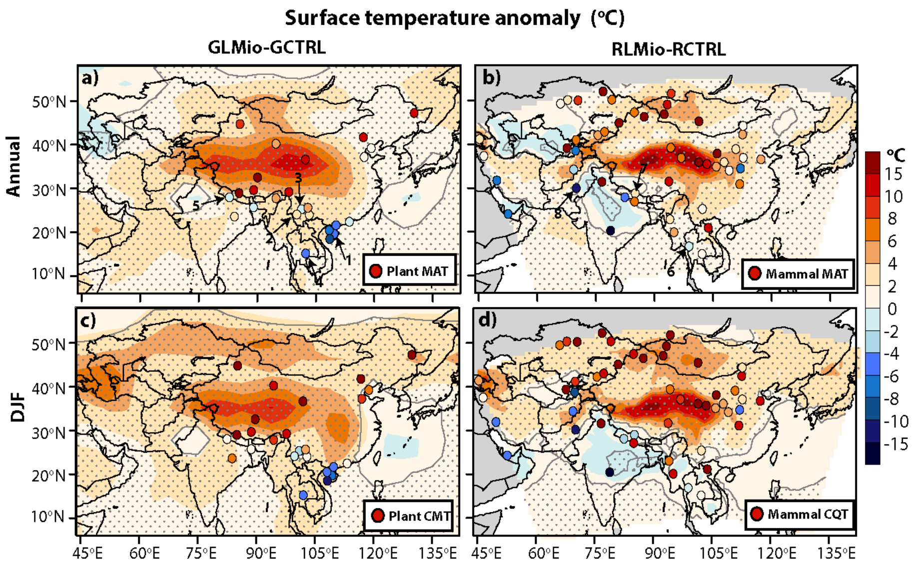

Figure 3. Temperature changes (°C) in the Late Miocene as indicated by proxy and climate models. Mean annual temperature: **(a)** GLMio-GCTRL, **(b)** RLMio-RCTRL. Mean winter temperature: **(c)** GLMio–GCTRL, **(d)** RLMio–RCTRL. The dotted area has temperature anomalies significant with a Student's t test ($p < 0.05$) in the models. The circles denotes the changes in mean annual temperature (MAT) in **(a)** and **(b)**, and coldest month (quarter) temperature, i.e., CMT (CQT), in **(c)** and **(d)**, as indicated by plant and mammal proxies. The arrows denote the fossil localities selected for Fig. 6: 1. Fushan, 2. Xiaolongtan, 3. Lühe, 4. Khorat, 5. Sural Khola, 6. Sop Mae Tham, 7. Jilong, 8. Zinda.

CPD
11, 63–93, 2015

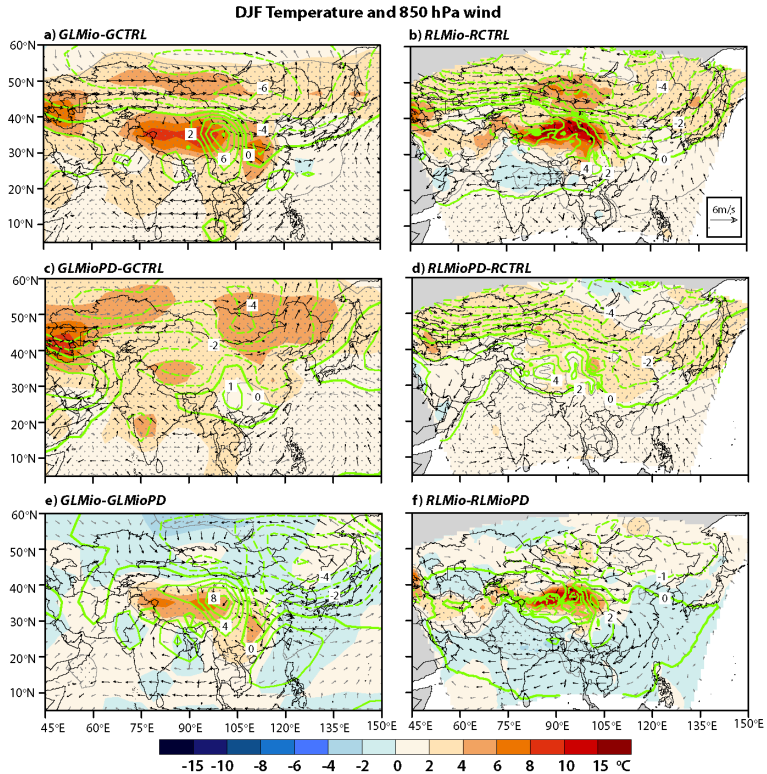

Figure 4. Winter temperature (°C) (shaded), 850 hPa wind ($m\,s^{-1}$) (vector) and sea level pressure (hPa) (contour) changes due to the Late Miocene Asian orography and other boundary condition changes. **(a)** GLMio-GCTRL, **(b)** RLMio-RCTRL, **(c)** GLMioPD-GCTRL, **(d)** RLMioPD-RCTRL, **(e)** GLMio-GLMioPD, **(f)** RLMio-RLMioPD. The solid (dashed) contours denote the positive (negative) pressure anomalies. The dotted areas (black vectors) denote temperature (wind) anomalies significant with a Student's t test ($p < 0.05$).

CPD
11, 63–93, 2015

Strong winter monsoon causes Miocene cooling

H. Tang et al.

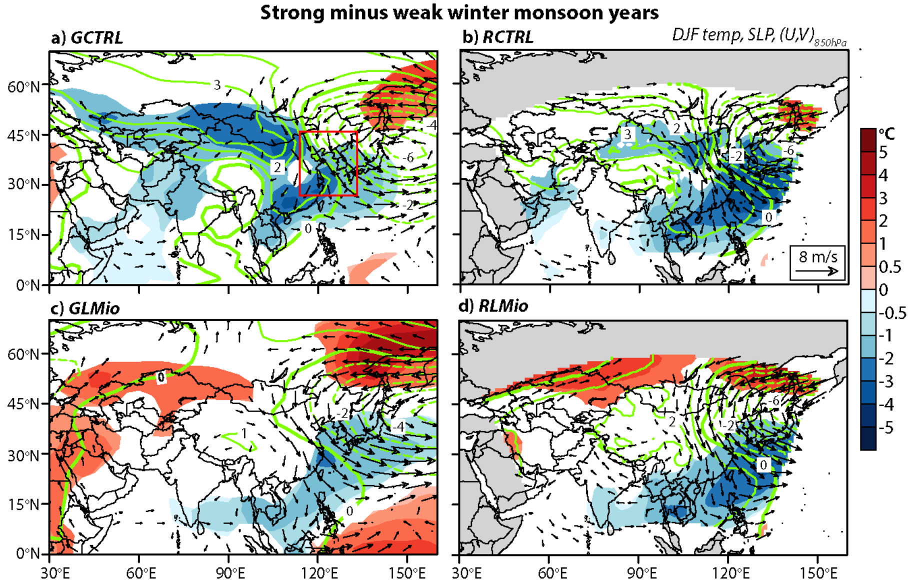

Figure 5. As that in Fig. 1a, but for the climate model experiments. **(a)** GCTRL, **(b)** RCTRL, **(c)** GLMio, **(d)** RLMio.

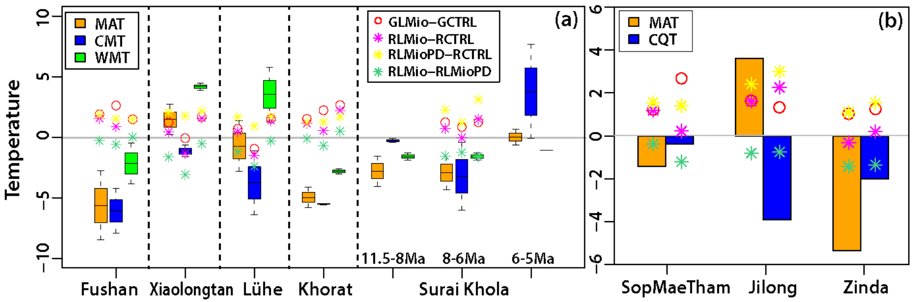

Figure 6. Model-proxy comparison at selected plant **(a)** and mammal **(b)** fossil localities indicated by numbers in Fig. 3. In **(a)**, the line in the box denotes the median value of plant fossil reconstruction, the box shows the 25–75 % range and the whiskers show the total range. In **(b)**, the height of the bar denotes the value estimated from mammal fossil data. The circle and asterisks denote the mean values of the global and regional model results, respectively. For the localities where the surface elevation is different between the two compared model experiments, the effect of elevation on surface temperature is removed by assuming a lapse rate of 6 °C km^{-1} to obtain the pure effect of winter monsoon on temperature changes. MAT: Mean annual temperature; CM(Q)T: Coldest month (quarter) temperature; WMT: Warmest month temperature.

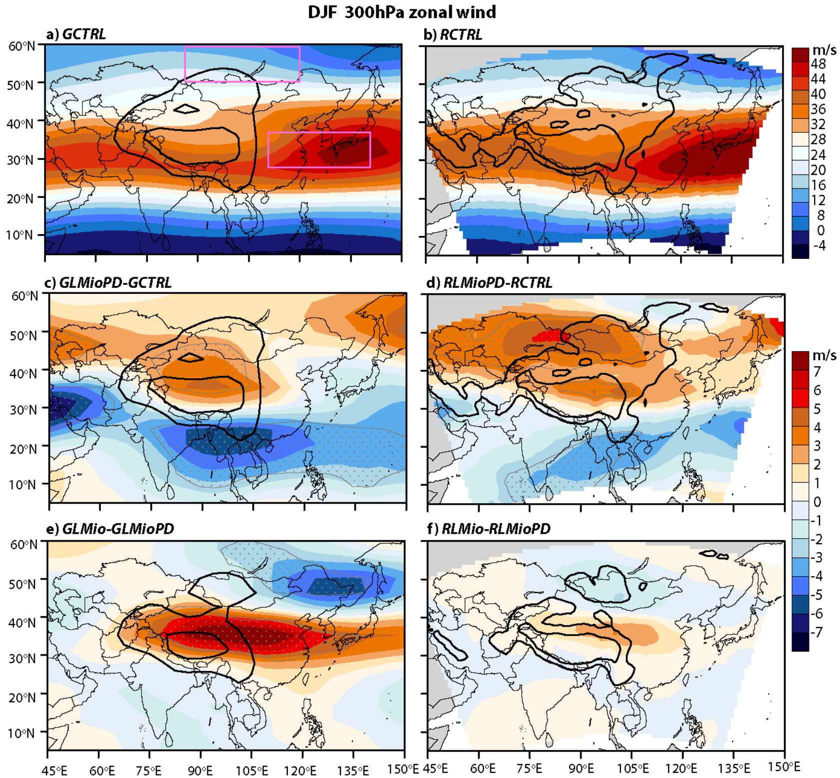

Figure 7. 300 hPa zonal wind in winter and its changes due to the Late Miocene Asian orography and other Late Miocene boundary conditions. **(a)** GCTRL, **(b)** RCTRL, **(c)** GLMioPD-GCTRL, **(d)** RLMioPD-RCTRL, **(e)** GLMio-GLMioPD, **(f)** RLMio-RLMioPD. The purple boxes in **(a)** denote the regions used to calculate winter monsoon index JS in Table 2. The black contours surround the regions with surface pressure lower than 700 and 900 hPa. The dotted areas denote wind anomalies significant with a Student's t test ($p < 0.05$).

CPD
11, 63–93, 2015